Redox Biology 2 (2014) 632–639

Contents lists available at ScienceDirect

Redox Biology

journal homepage: www.elsevier.com/locate/redox

Research Paper

SOD1 oxidation and formation of soluble aggregates in yeast: Relevance to sporadic ALS development

Dorival Martins, Ann M. English*

Department of Chemistry and Biochemistry, Concordia University, 7141 Sherbrooke West, Montreal, Quebec, Canada H4B 1R6

ARTICLE INFO

Article history:
Received 24 March 2014
Accepted 24 March 2014

Keywords:
Wild-type Sod1
Oxidative PTMs
Soluble aggregates
Sporadic ALS
Yeast

ABSTRACT

Misfolding and aggregation of copper–zinc superoxide dismutase (Sod1) are observed in neurodegenerative diseases such as amyotrophic lateral sclerosis (ALS). Mutations in Sod1 lead to familial ALS (FALS), which is a late-onset disease. Since oxidative damage to proteins increases with age, it had been proposed that oxidation of Sod1 mutants may trigger their misfolding and aggregation in FALS. However, over 90% of ALS cases are sporadic (SALS) with no obvious genetic component. We hypothesized that oxidation could also trigger the misfolding and aggregation of wild-type Sod1 and sought to confirm this in a cellular environment. Using quiescent, stationary-phase yeast cells as a model for non-dividing motor neurons, we probed for post-translational modification (PTM) and aggregation of wild-type Sod1 extracted from these cells. By size-exclusion chromatography (SEC), we isolated two populations of Sod1 from yeast: a low-molecular weight (LMW) fraction that is catalytically active and a catalytically inactive, high-molecular weight (HMW) fraction. High-resolution mass spectrometric analysis revealed that LMW Sod1 displays no PTMs but HMW Sod1 is oxidized at Cys146 and His71, two critical residues for the stability and folding of the enzyme. HMW Sod1 is also oxidized at His120, a copper ligand, which will promote loss of this catalytic metal cofactor essential for SOD activity. Monitoring the fluorescence of a Sod1-green-fluorescent-protein fusion (Sod1-GFP) extracted from yeast chromosomally expressing this fusion, we find that HMW Sod1-GFP levels increase up to 40-fold in old cells. Thus, we speculate that increased misfolding and inclusion into soluble aggregates is a consequence of elevated oxidative modifications of wild-type Sod1 as cells age. Our observations argue that oxidative damage to wild-type Sod1 initiates the protein misfolding mechanisms that give rise to SALS.

Introduction

Copper–zinc superoxide dismutase (Sod1) is an abundant, ubiquitous enzyme found in the cytosol [1], mitochondria [1,2] and nucleus [1] of eukaryotic cells. It is critical in the detoxification of superoxide radicals produced during aerobic respiration and its deletion renders eukaryotes hypersensitive to oxygen [3]. The biophysical properties of Sod1 have been extensively studied since its misfolding and aggregation are associated with the development of late-onset neurodegenerative diseases such as Parkinson's, Alzheimer's and Amyotrophic Lateral Sclerosis (ALS) [4,5]. Notably, close to 180 ALS-associated mutations have been reported in the human *SOD1* gene [6] and neurotoxicity is linked to their structural instability. The ALS mutant proteins appear more prone than wild-type Sod1 to aggregation into high molecular weight structures that form non-amyloid aggregates [4,6–8], a hallmark of ALS [8,9]. However, 90% of ALS cases are not linked to any known genetic mutation and are classified as sporadic ALS (SALS). The protein misfolding mechanisms underlying the development of SALS and FALS remain poorly understood. Human Sod1 was demonstrated to have prion-like properties that can trigger its aggregation [10], but ALS may be distinct from other late-onset neurodegenerative diseases [4] in that non-amyloid aggregates contribute to its development [11–13].

Oxidative damage is generally implicated in the misfolding of Sod1 mutants that cause FALS [11–13] and oxidized proteins accumulate during cell aging [14,15]. Paradoxically, its dismutase activity that forms H_2O_2 as a product may render Sod1 more susceptible to oxidative PTMs than other proteins [7,8]. The redox-active catalytic Cu center of Sod1 displays pseudoperoxidase activity and exposure of the enzyme to excess H_2O_2 *in vitro* results in selective oxidation of Cu-coordinating residues with loss of catalytic activity and oligomerization [7,8,16,17] by mechanisms that have not been fully elucidated [18,19]. Cu is ligated to His46, His48, His120 and His63, which bridges Cu to the Zn cofactor (Fig. 1). Zn is additionally coordinated to His71, His80 and Asp83 (Fig. 1), and plays an important structural role that stabilizes the Sod1 homodimer [8]. Cys57 and Cys146 form an intra-subunit disulfide that facilitates coordination of the histidine residues

* Corresponding author.
E-mail address: ann.english@concordia.ca (A.M. English).

http://dx.doi.org/10.1016/j.redox.2014.03.005

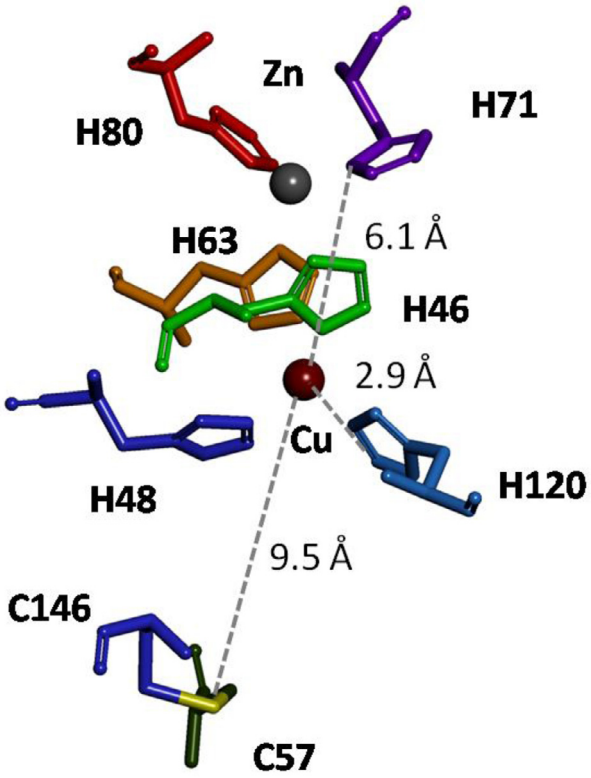

Fig. 1. Active-site residues in Sod1. The catalytic Cu cofactor is coordinated to His46, His48, His120 and bridging His63. The structural Zn cofactor is coordinated to His63, His71 and His80 as well as aspartic acid Asp83 (not shown). The intrasubunit disulfide bridge between Cys57 and Cys146 is important in stabilizing the Sod1 homodimer [7,8,20]. The distances from Nϵ of His120 and His71, and the Cys57–Cys146 disulfide bridge to the catalytic Cu (2.1, 6.9 and 9.5 Å, respectively) were measured in the 1.15-Å resolution crystal structure of human Sod1 (PDB 2V0A).

to the metal cofactors and also stabilizes the enzyme [8]. Thus, oxidation of a Zn ligand with loss of the metal [11,20] or disruption of the Cys57–Cys146 disulfide destabilize the enzyme and promote its aggregation [20]. Since wild-type Sod1 is oxidized by H_2O_2 *in vitro* [16,21], this could also occur *in vivo*. Increased oxidative stress has been associated with both FALS and SALS [4,22], and increased protein oxidation has been detected by OxyBlot in transgenic mouse models of ALS [4,22,23]. However, oxidized Sod1 does not accumulate in the livers of aging rats [24], so despite strong links between oxidative stress and ALS, oxidative PTMs in Sod1 have not been correlated with pathogenicity.

Liver protein turnover is relatively rapid so modified protein accumulation in this organ may be less than in other tissues. Thus, in order to probe for specific sites of Sod1 oxidation in an aging cellular environment, we selected stationary-phase yeast. In this state, yeast cells are non-dividing [25] and in this respect resemble other quiescent cells such as motor neurons [26–29]. However, yeast rapidly age [25], which allows protein modification to be examined over a cell's lifespan in a matter of weeks rather than years. Furthermore, yeast and human Sod1 share 70% homology and over 90% identity in their active-site residues.

We report here that distinct populations of Sod1 exist in stationary-phase yeast. A low molecular weight, catalytically active fraction with the mass (~32 kDa) of the native Sod1 dimer (LMW Sod1) and a soluble, high molecular weight, catalytically inactive fraction, with a mass over 300 kDa (HMW Sod1). High-resolution mass spectrometry (MS) revealed negligible oxidation in LMW Sod1 but HMW Sod1 was oxidized at residues critical for SOD activity and enzyme stability, suggesting that oxidative damage may trigger Sod1 inclusion into soluble HMW aggregates. Furthermore, HMW Sod1-GFP levels increased dramatically in old yeast chromosomally expressing this fusion, pointing to increased Sod1 oxidation with age. The possible relevance of oxidative PTM of Sod1 in SALS development is discussed.

Materials and methods

Yeast strains, media, and growth conditions

The BY4741 *Saccharomyces cerevisiae* strains used in this study are listed in Table 1. Wild-type BY4741 was purchased from the European *S. cerevisiae* Archive for Functional Analysis (EUROSCARF, Frankfurt, Germany). The BY4741 strain expressing chromosomal *SOD1* C-terminally tagged with green fluorescent protein was kindly provided by Prof. Christopher Brett (Department of Biology, Concordia University). The two strains were grown in YPD liquid medium (1% yeast extract, 2% peptone and 2% glucose) at a flask-to-medium volume ratio of 1:5. The cultures at an initial $OD_{600} = 0.01$ were incubated at 30 °C with shaking at 225 rpm. The spent YPD medium was replaced with 0.85% NaCl solution (w/v) after 72 h to switch cells to stationary phase, a quiescent, non-dividing state [26–28].

Preparation of soluble protein extracts

These were prepared as previously described [30]. Cells were collected at 2000*g*, washed twice with 20 mM potassium phosphate buffer (KPi, pH 7.0) containing 0.1 mM PMSF, the pellets were suspended in the same buffer ±0.1 M iodoacetamide, and mixed with an equal volume of acid-washed glass beads. Cell suspensions were vortexed (4 × 15 s cycles), cell debris was removed by centrifugation at 13,000*g* for 10 min at 4 °C, and the total protein concentration in the supernatants (i.e., the soluble protein extracts) was determined by the Bradford assay with bovine serum albumin as a standard [31].

Fractionation of soluble protein extracts by size-exclusion chromatography (SEC)

Extracts from wild-type and Sod1-GFP-producing yeast strains were fractionated by SEC on a Superose 12 HR 10/30 column (Amersham; total volume 25 mL; void volume 7 mL; fractionation range 1–300 kDa) coupled to an ÄKTApurifier 10. The SEC column was equilibrated with 20 mM KPi/300 mM NaCl (pH 7.0), 1 mL of extract (0.1–0.4 mg total protein) in 20 mM KPi (pH 7.0) was loaded on the column, proteins were eluted with the equilibration buffer at a flow rate of 0.3 mL/min, and detected spectrophotometrically at 280 nm. SEC fractions of 1 mL were collected and probed for Sod1 by SOD activity assay and immunodot blotting. Extracts containing Sod1-GFP were analyzed using the same Superose 12 HR column attached to an Agilent 1100 HPLC with a fluorescence detector to monitor GFP in the eluate (ex/em 470/520 nm).

In-gel SOD activity assay

SOD activity in the SEC fractions was assayed in native polyacrylamide gels to separately measure the activity of the Sod1 and Sod2 isoforms present in yeast [32]. The unfractionated soluble protein extracts and the SEC fractions containing 1–5 μg total protein were electrophoresed in 12% resolving gels at 50 mA for 2 h at 4 °C. The gels were incubated for 30 min at 20 °C in the dark with a staining solution (0.17 mM NBT, 6.7 mM TEMED and 0.3 mM riboflavin in 100 mM KPi, pH 7.2), rinsed twice with distilled water and exposed to white light from a 60-W mercury lamp for 60 min, and scanned on an AlphaImager (AlphaInnotec) to quantify the optical densities of the negative bands containing SOD activity by ImageJ software.

Table 1
S. cerevisiae strains used in this study.

Strain	Description	Reference
Wild-type BY4741	*MATa his3Δ1 leu2Δ0 met15Δ0 ura3Δ0*	EUROSCARF
Sod1-GFP expressing strain	BY4741 cells with *SOD1-GFP*	This work

Immunodetection of Sod1 in the SEC fractions

These fractions were probed for Sod1 protein in immunodot blots. Briefly, a 10 μL drop of the unfractionated soluble protein extract or of a SEC fraction containing 5–20 μg protein was spotted onto a methanol-soaked PVDF membrane and allowed to dry for 10 min at room temperature. The membrane was blocked for 1 h in TBST (50 mM Tris, 150 mM NaCl and 0.05% Tween 20 v/v, pH 7.6) containing 5% skimmed milk (w/v), and incubated with rabbit anti-human Sod1 antibody (Stressgen; dilution 1:1000) in 1% milk/TBST for 3 h at room temperature. After washing with TBST, the membrane was incubated for 1 h with goat anti-rabbit HRP-conjugated secondary antibody (BioRad; dilution 1:10,000) diluted in 1% milk/TBST. Sod1-containing peaks were detected by chemiluminescence using an ECL kit (Thermo, Fisher) and the membrane was scanned on the AlphaImager.

SDS-PAGE and trypsin digestion of SEC fractions

The SEC fractions containing Sod1 protein were decomplexified by 1D SDS-PAGE under reducing conditions on 6% stacking and 12% resolving gels. After 1 h electrophoresis at 120 V, the gels were Coomassie stained and slices were excised between the 10 and 25-kDa MW markers that bracket the mass of the Sod1 monomer (16 kDa). In this mass range, we selected for aggregates stabilized by non-covalent bonds (disulfides were reduced) to maximize sequence coverage by mass spectrometry as discussed below. Following destaining with 5% acetonitrile in 50 mM aqueous ammonium bicarbonate (pH 7.5), proteins in the gel slices were reduced with 10 mM DTT for 30 min at 60 °C, and alkylated with 55 mM iodoacetamide for 30 min at room temperature. The gel slices were separately incubated overnight with trypsin at 37 °C and the peptides were extracted from the gel slices with 60% acetonitrile in 50 mM aqueous ammonium bicarbonate (pH 7.5) for analysis by LC–MS.

LC–MS screening for oxidative PTMs in Sod1

Tryptic peptides (5 μL/injection) were separated on a home-made reversed-phase C18 column (0.75 μm ID × 7.5 cm) attached to an Easy-nLC 1000 (Thermo Scientific) using a 2–94% acetonitrile gradient in 0.1% aqueous formic acid at a flow rate of 200 nL/min. The nanoLC output was directed into the ESI source of an LTQ Orbitrap Velos mass spectrometer (Thermo Scientific) and analyzed in full-scan mode using the Orbitrap high resolution mass analyzer (m/z range 350–3000; resolution 60,000 at m/z 400). Other MS parameters were: electrospray voltage 3 kV, CID collision energy 30 V and heated capillary temperature 200 °C. Precursor ions of the Sod1 peptides were selected using a mass exclusion threshold of 10 ppm and subjected to MS/MS in the Velos linear ion trap mass analyzer using a mass tolerance of 0.8 u for the fragment ions. MS/MS fragments with an intensity count of 20 or greater were analyzed using Proteome Discoverer 1.3.0 (Thermo Scientific) and the Sequest search engine with mass filters for oxidation (+16, +32, +48 u) of Met, Cys, Trp, Tyr; and Cys alkylation by iodoacetamide (+57 u) or acrylamide (+71 u). Sequest correlated the MS/MS spectra with peptide sequences in the yeast proteome database downloaded from the NCBI website (*ftp://ftp.ncbi.nlm.nih.gov/*). For confident identification of Sod1, the following Sequest filters were implemented: Score > 30, XCorr ≥ 2, False Discovery Rate < 0.01 and a minimum of two unique peptides. The Score is the probability that the identified protein is a correct match based on a comparison of its experimental and theoretical MS/MS spectra. XCorr is the cross-correlation between the theoretical and experimental MS/MS spectra of the sequenced peptides. Unique peptides are those present in Sod1 only and absent from all other proteins in the yeast database. Table S1 lists the precursors ion analyzed by MS/MS and Tables S2–S4 (Supplementary Information) summarize the *b* and *y* sequence used to assign the PTMs.

Results

Catalytically inactive Sod1 is present in HMW fractions from the SEC column

SEC fractionation of the soluble protein extract from 7-day yeast cells yielded four resolved chromatographic peaks (P1–P4, Fig. 2A) and shoulders appear on P3 and P4. Peak P1 is eluted within the void volume of the column (7 mL) and hence contains soluble protein complexes or aggregates > 300 kDa, the upper limit of the fractionation range of the Superose column. P2, P3 and P4 are eluted at 12, 18 and 20 mL, respectively, and contain increasingly smaller soluble proteins. SOD activity was detected only in the extract and P3 (Fig. 2B, upper panel) but immunodot blotting reveals the presence of Sod1 protein in the extract, P1, P1′ (7 and 7.5 mL, respectively) and P3 (Fig. 2B, lower panel). Hence, stationary-phase yeast cells contain HMW catalytically inactive populations of soluble Sod1 in addition to the expected LMW catalytically active enzyme.

HMW Sod1 is oxidized at Cys146, His120 and His71

To determine if PTMs are present in HMW Sod1, we examined aliquots of P1 by LC–MS with high mass resolution ($R = 60{,}000$) and high mass accuracy (<10 ppm). The P1 and P1′ fractions in the immunodot blot (Fig. 2B, lower panel) both come from the single unresolved SEC peak, P1 (Fig. 2) and were combined for further analysis. The SEC peak P1 was subjected to 1D SDS-PAGE under reducing conditions (0.7 M 2-mercaptoethanol) (Fig. 3), slices were excised from the gel, and following in-gel protein digestion, the tryptic peptide mixtures were extracted and analyzed by LC–MS/MS. The LWM Sod1 SEC fraction (P3) was treated in the same manner and a representative SDS-PAGE gel in shown in Fig. 3. Sod1 identification by LC–MS of its tryptic peptides gave high confidence Scores and ≥77% sequence coverage (Table 2).

Sod1 peptides were present in two gel slices cut from lane P1 close to the expected MW of the Sod1 monomer (16 kDa) (Fig. 3, red squares). This suggests that treatment with SDS detergent converts HMW Sod1 into LMW species under reducing conditions. Nonetheless, a fraction of HMW Sod exhibits aberrant migration in SDS-PAGE since peptides from LMW Sod1 were detected only in the gel slice cut from lane P3 below the 15 kDa MW marker (Fig. 3). As expected, LMW Sod1 migrates within the mass range (14–17 kDa) reported for the native yeast Sod1 monomer in SDS-PAGE gels [33]. Notably, no Sod1 peptides were reliably detected in gel slices containing proteins with an apparent MW > 30 kDa (data not shown).

Table 2
LC–MS analysis of Sod1 peptides in P1 and P3[a].

Sample	P1 (R15)	P1 (R25)	P3 (R15)
Score[b]	171	85	96
% Sequence coverage[c]	77	84	94
Unique peptides[d]	11/15	12/15	13/15

[a]The soluble proteins were extracted from three independent cultures, fractionated by SEC (Fig. 2A) and SDS-PAGE (Fig. 3), in-gel digested with trypsin and analyzed by LC–MS. P1 and P3 refer to the Sod1-containing SEC peaks in Fig. 2A; R15 and R25 refer to the marked regions of the SDS-PAGE gel in Fig. 3. This table provides representative results from the three cultures.
[b]The score calculated by the Proteome Discoverer software is the probability that the identified protein is a correct match based on a comparison of its experimental and theoretical MS/MS spectra. Scores were in the range of 65–171 for the three independent experiments.
[c]The % sequence coverage corresponds to the number of residues in all the Sod1 peptides detected by MS divided by 154 residues in yeast Sod1. Sequence coverage was in the range of 68–94% for the three independent experiments.
[d]Unique peptides are those present in Sod1 only and absent from all other proteins in the NCBI yeast database (ftp://ftp.ncbi.nlm.nih.gov/).

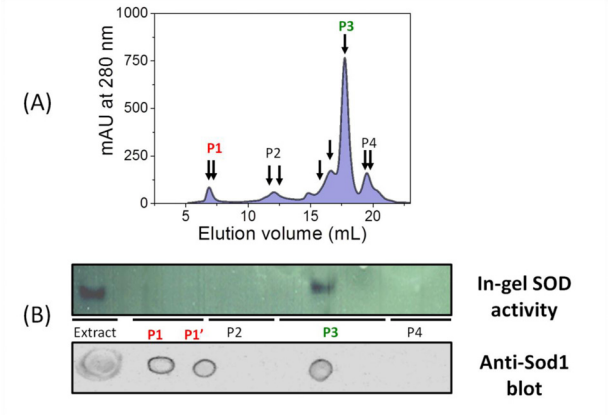

Fig. 2. SEC reveals the presence of HMW and LMW Sod1 populations in the soluble protein extract from 7-day stationary-phase yeast cells. (A) Size exclusion chromatogram of the extract. A 100-μL aliquot of extract containing 0.4 mg of protein was diluted to 1 mL with 20 mM KPi (pH 7.0) and loaded on a Superose 12 HR 10/30 column (1.0 cm × 30 cm) equilibrated with 20 mM KPi/300 mM NaCl (pH 7.0) and connected to the ÄKTApurifier. Proteins were eluted with the equilibration buffer at a flow rate of 0.3 mL/min and detected at 280 nm. The arrows indicate the fractions that were tested for immunoreactivity and SOD activity. (B) Upper panel: in-gel Sod1 activity following native PAGE of the extract and the SEC fractions each containing 1 μg of total protein. Bands were stained with riboflavin as a superoxide generator and NBT, which is reduced to formazan in the presence of superoxide [32]. (B) Lower panel: Sod1 protein was detected by immunodot blot in the extract, two fractions of the SEC column void volume P1 (7 mL) and P1′ (7.5 mL), and in P3 (18 mL). Samples containing 10 μg of protein were dotted onto PVDF membranes and probed with rabbit anti-human Sod1 antibody. See "Materials and methods" section for additional information. Sod1 that was eluted in P1, P1′ and in P3 is referred to in the text as HMW Sod1 and LMW Sod1, respectively. P1 and P1′ were combined and treated as a single P1 fraction for LC–MS analysis. Proteins were extracted from three independent cultures and representative results are presented here.

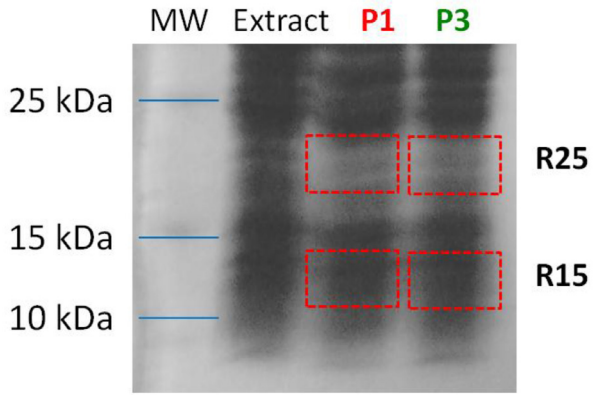

Fig. 3. Decomplexation of Sod1-containing SEC fractions by SDS-PAGE. Aliquots (25 μL) of the **P1** and **P3** SEC fractions from Fig. 2A containing 20 μg of protein were analyzed by reducing SDS-PAGE. Bands were excised from lanes P1 to P3 of the gel and subjected to in-gel tryptic digestion. Digests from the R15 and R25 regions (denoted by the red boxes) gave the highest score and Sod1 sequence coverage so Tables 2 and 3 summarize the LC–MS/MS results for these regions. Extracts from three independent cultures were analyzed and the gel shown is representative of the three. Blue lines indicate the centers of the MW markers, which are poorly visible in the scanned gel (lane MW).

We next examined the Sod1 tryptic peptides for PTMs. LMW Sod1 peptides were alkylated at cysteine residues by the added iodoacetamide and by trace acrylamide in the gel. They were also oxidized at methionine residues but this likely occurs during sample processing since we frequently find oxidized methionine in peptides and in intact proteins analyzed by LC–MS. Importantly, no peptide derivatives were found in LMW Sod1 that we could attribute to PTMs. Thus, we assume that LMW Sod1 was not oxidized *in vivo*, consistent with its retention of SOD activity (Fig. 2B). In contrast, Cys146 is oxidized to the sulfonic acid in HMW Sod1 (Fig. 4A; Table S1) that migrates below the 15 kDa marker in SDS-PAGE (Fig. 3). Although Cys146 and Cys57 form an intrasubunit disulfide bond in native mature Sod1, we did not detect Cys57 modification in the samples analyzed. Cys146 was also oxidized in HMW Sod1 from the iodoacetamide-treated lysates (Table 3) but alkylated in the corresponding LMW Sod1 sample. Hence, we conclude that Cys146 oxidation is a Sod1 PTM that occurs in intact cells and is not an artifact of sample preparation.

Aberrantly migrating HMW Sod1 cut from lane P1 of the gel above the 15 kDa marker (Fig. 3) was also found to be oxidized. However, in this fraction, the targets are His120 and His71 rather than cysteine. In fact, the Cu ligand His120 is 100% oxidized to oxo-histidine (Fig. 4B), which would explain the lack of SOD activity in P1 (Fig. 2B, upper panel) since H_2O_2 exposure of purified Sod1 in solution results in oxidation of the Cu ligands His46, His48 and His120, and loss of SOD activity [16,17,21]. The Zn ligand, His71, is additionally 100% oxidized to oxo-histidine in this fraction (Fig. 4C; Table S1), which would have decreased the protein's affinity this metal cofactor. Critically, loss of Zn destabilizes the homodimer interface of Sod1 and results in monomer aggregation *in vitro* [20]. Hence, His71 oxidation *in vivo* could have triggered the formation of the HMW Sod1 found in P1 (Fig. 2A). We conclude that there are differential mechanisms of Sod1 oxidation in stationary-phase yeast that result in its oxidation at Cys146, His120 or His71. These PTMs result in loss of catalytic activity and in the formation of soluble HMW Sod1-containing aggregates that are disrupted by detergent under reducing conditions.

Screening for HMW Sod1 as yeast cells age

Since ALS and other neurodegenerative diseases are late-onset [4,6,7], we questioned if HMW Sod1 accumulation increased during yeast aging. Thus, we monitored Sod1-GFP fluorescence in SEC fractions from stationary-phase yeast cells expressing this fusion protein over several weeks. HMW Sod1-GFP fluorescence in P1 corresponds

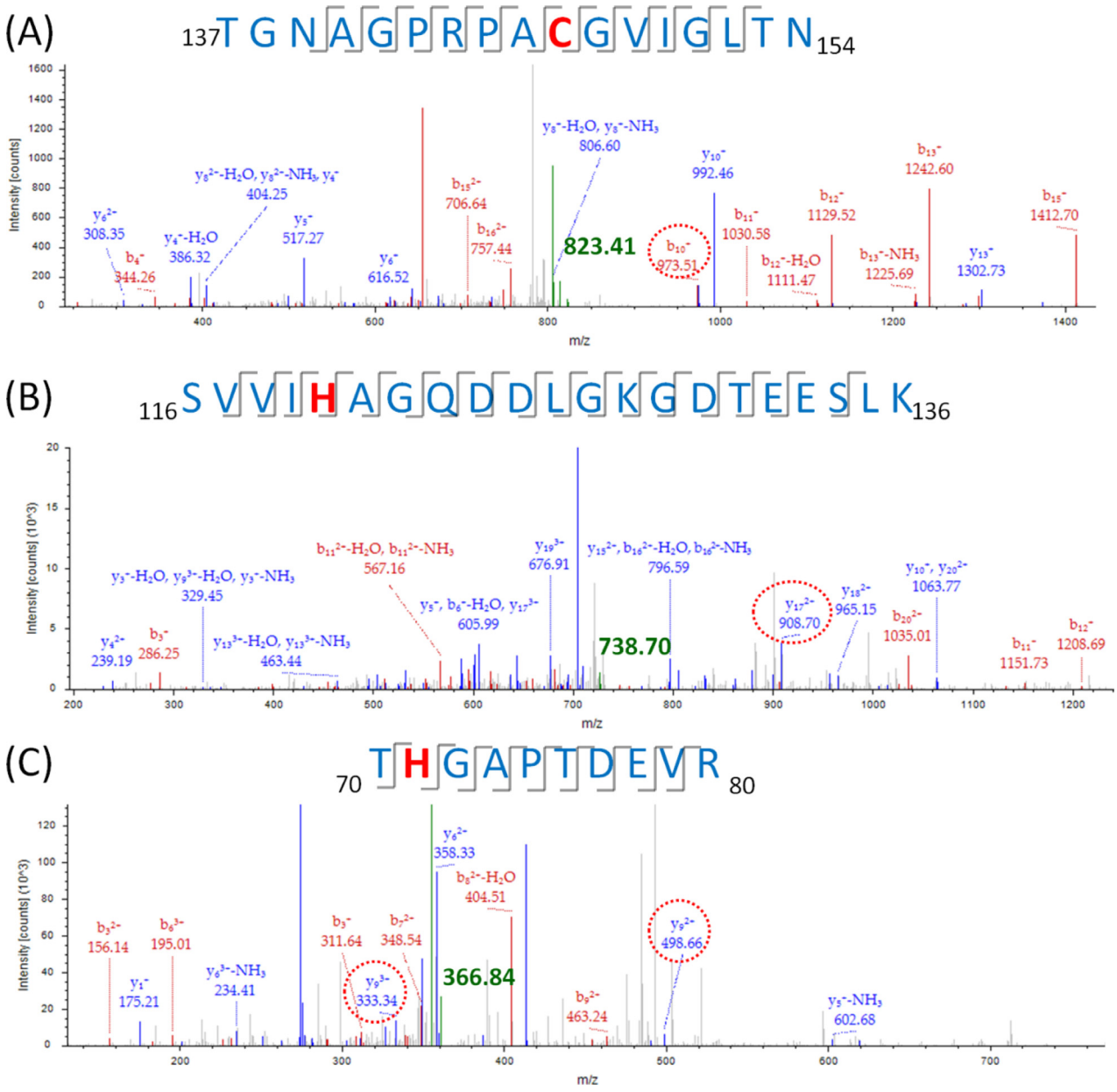

Fig. 4. HMW Sod1 is oxidized at Cys146, His71 and His120. MS/MS spectrum of the (A) $(M + 2\ H)^{2+}$ ion at m/z 823.41 of the C-terminal peptide containing Cys146-SO_3H; (B) $(M + 3\ H)^{3+}$ ion at m/z 738.70 of the oxo-His120 peptide; and (C) $(M + 3\ H)^{3+}$ ion at m/z 366.84 of the oxo-His71 peptide. The peptide (precursor) ions (green) (see Table S1 and sequence above spectra) were fragmented by CID (30 V) to give *b* (red) and *y* sequence ions (blue). The smallest visible *b* or *y* ion bearing the modified residue (see Tables S2–S4) is circled in each spectrum. The peptide ion match (number of $y + b$ ions identified in the MS/MS spectrum divided by the theoretical number of $y + b$ ions generated by CID) is (A) 18/32, (B) 22/80, and (C) 13/36. The XCorr values are (A) 2.5, (B) 2.0 and (C) 2.0. The MS operating parameters are given in the "Materials and methods" section.

to 0.2% of the total Sod1-GFP fluorescence in the SEC fractions as cell begin to enter stationary phase (day 3, Fig. 5A). However, this value climbs to 8%, a 40-fold increase, in 30-day cells before dropping significantly in 40- and 52-day cells (Fig. 5B). Thus, Sod1-GFP aggregation increases as cell age but HMW Sod1-GFP may be converted in very old cells into insoluble aggregates that would be pelleted prior to SEC fractionation.

Discussion

A fraction of Sod1 is present in HMW aggregates and possesses oxidative PTMs in 7-day, stationary-phase yeast cells (Fig. 4; Table 3). Within these aggregates Sod1 is catalytically inactive and oxidized at Cys146 or His71 and His120 (Fig. 4). These three residues are critical for the folding and stability of the Sod1 homodimer, and their oxidation likely triggers formation of HMW Sod1 that is readily isolated from the soluble protein extracts by SEC (Fig. 2).

The intrasubunit Cys146–Cys57 disulfide (Fig. 1) is essential in stabilizing the active site of Sod1 by orienting the coordinating ligands towards the Cu and Zn cofactors [34]. Notably, Cys146–SO_3H (human Sod1 numbering) was isolated from Parkinson's and Alzheimer's brains [5], and inactive Sod1 from the airway epithelia of asthmatic patients displays disruption of the Cys146–Cys57 disulfide [35]. Since disulfides are more resistant to oxidation than thiols, Cys146 may undergo oxidation in immature Sod1 prior to Cys146–Cys57 disulfide formation. In addition to destabilizing the dimer, such oxidation would decrease the SOD activity of cells since the ALS Sod1 C146R variant has <10% of wild-type activity [8]. Curiously, we did not detect oxidized Cys57, the disulfide partner of Cys146 (Fig. 1), although

Table 3
Summary of oxidative modifications found in HMW Sod1 from 7-day yeast cells[a].

	SDS-PAGE R15 region	SDS-PAGE R15 region + IA	SDS-PAGE R25 region	SDS-PAGE R25 region + IA
% Sequence coverage[b]	77	78	84	74
Cys146[c]	SO_3H	SO_3H	P[d]	A/P[d]
His120[c]	None	None	Oxo-His	Oxo-His
His71[c]	None	None	Oxo-His	Oxo-His

[a]The soluble proteins were extracted from three independent cultures, fractionated by SEC (Fig. 2A) and SDS-PAGE (Fig. 3), in-gel digested with trypsin and analyzed by LC–MS. P1 and P3 refer to the Sod1-containing SEC peaks in Fig. 2A; R15 and R25 refer to the marked regions of the SDS-PAGE gel in Fig. 3. This table provides representative results from the three cultures.
[b]The % sequence coverage corresponds to the number of residues in all the Sod1 peptides detected by MS divided by 154 residues in yeast Sod1. Sequence coverage was in the range of 68–94% for the three independent experiments.
[c]PTMs at these residues detected in the MS/MS spectra of tryptic peptides (Fig. 4) from HMW Sod1 present in the R15 or R25 region of the SDS-PAGE gel (Fig. 3). MS/MS spectra were recorded only for precursor ions found in LC-MS spectra (data not shown) that resulted in >70% sequence coverage.
[d]A/P, acetamide and propionamide adducts formed on reaction of cysteine sulfhydryl with iodoacetamide (IA) when added before cell lysis or with free acrylamide present in the gels during SDS-PAGE.

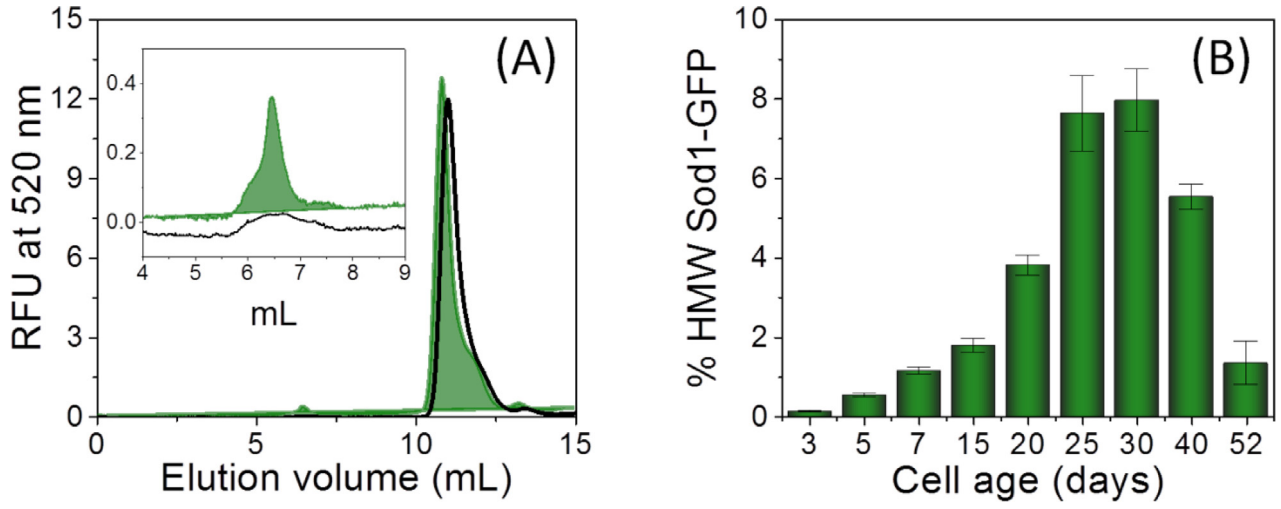

Fig. 5. HMW Sod1-GFP accumulates as yeast age but declines in very old cells. Soluble protein extracts from cells chromosomally expressing Sod1-GFP were fractionated by SEC as described in the legend of Fig. 2 except that the Superose column was coupled to an Agilent 1100 HPLC with a fluorescence detector, and GFP fluorescence was monitored with ex/em 470/520 nm. (A) Size-exclusion chromatogram of extracts from 3- (black line) and 7-day (green area) cells. LMW Sod1-GFP is present in the intense peaks centered at ~11 mL and the inset shows a 100-fold expansion of the HMW Sod1-GFP fractions at 6.5 mL. (B) Variation with cell age of HMW Sod1-GFP as a percentage of the total peak area.

both cysteines are mutated in FALS [6].

Oxidation of the histidines that bind Sod1's metal cofactors (Fig. 1) will labilize the metals. Three of the four copper ligands, His46, His48 and His120 (Fig. 1) that are mutated in FALS [6] are found to be oxidized in H_2O_2-treated Sod1 *in vitro* [21]. Curiously, His120 is the only Cu ligand we find oxidized in our soluble HMW Sod1 fraction isolated from yeast (Fig. 4B). Although no Zn ligands were found be oxidized by H_2O_2 *in vitro* [21], we discovered that His71, which is not a reported mutation site in FALS [6], is a target of oxidative modification in yeast (Fig. 4C). Hence, oxidative PTMs could labilize both metal cofactors in Sod1 and promote its aggregation since Cu loss during acid denaturation increases the enzyme's kinetic instability [36] and Zn loss promotes subunit aggregation *in vitro* [20].

A copper-bound hydroxyl radical formed during the pseudoperoxidase activity of Sod1 may mediate oxidation of a copper ligand such as His120 [17]. In contrast, a diffusible oxidant such as copper released from the oxidized enzyme or a carbonate radical formed by the pseudoperoxidase activity [18,19] in presence of physiological CO_2 levels likely oxidizes His71 at 6.1 Å from copper (Fig. 1). Notably, we find that both His120 and His71 are present as oxo-histidine in the same HMW Sod1 fraction, suggesting that these oxidations are somehow coupled. However, Cys146 oxidation is observed in a different HMW Sod1 fraction, which we proposed above may arise from immature metal-free Sod1. Although we identified three sites of oxidative PTMs in Sod1 from aged yeast, it is important to emphasize that the protein may undergo more PTMs. Our current methodology is selective for soluble aggregates stabilized by non-covalent interactions (Figs. 2A and 3). Additional oxidative PTMs may trigger the formation of aggregates stabilized by covalent interactions that would migrate slowly during SDS-PAGE or of insoluble aggregates that would be pelleted with cell debris.

Neurotoxicity has been associated with the borderline stability that results in the conversion of Sod1 variants into non-amyloid aggregates [4]. However, a FALS-causing human Sod1 mutant with wild-type stability has recently been identified [37], suggesting that additional genetic and/or environmental factors are responsible for SALS induction. Clearly, HMW Sod1-GFP sharply increases during the chronological aging of yeast (Fig. 5B), which may reflect increased oxidative damage to the protein as anticipated in old cells [14]. But if Sod1 oxidation occurs during normal cell aging, what triggers soluble HMW Sod1 aggregates to become toxic to motor neurons? This may involve accumulation of the aggregates in mitochondria followed by respiratory dysfunction [4,38], co-aggregation of Sod1 with transcription factors necessary for neuronal survival [4] or membrane disruption [4]. A cell's capacity to degrade misfolded Sod1 or to immobilize soluble aggregates into insoluble forms may additionally control the accumulation of toxic species.

Strengths and limitations of the yeast model

The mechanisms underlying the development of SALS remain unclear but are likely multiple and heterogeneous [7,8]. Of the three sites of oxidative PTMs that we identify in Sod1 from stationary-phase yeast, only a Cys146 FALS mutant (C146R) has been described [6]. Also, oxidation of His71 by H_2O_2 has not been reported *in vitro*. Thus, our work has identified an unexpected oxidative PTM in Sod1 from yeast and has additionally suggested two possible independent mechanisms of Sod1 aggregation involving Cys146 oxidation in the immature protein, and His71 plus His120 oxidation of the mature protein.

Although disulfide cleavage and metal cofactor release [7,8] are associated with human Sod1 aggregation and ALS, it is critical to establish if the PTMs observed here are relevant to disease development. Sod1 has a highly conserved active site, but human and yeast Sod1 possess only 70% sequence identity. Thus, we will examine PTMs in human Sod1 from yeast expressing this protein. Another critical issue is to distinguish between normal and pathological Sod1 aggregation with age as well as the sequestering of other essential proteins by Sod1 aggregates. To this end we will express aggressive Sod1 FALS mutants in yeast and examine their PTMs and their aggregates over time. Stationary-phase yeast cells are in a quiescent, non-dividing state like neurons [26] and exhibit the protein misfolding seen in neurodegenerative diseases such as ALS [39] and Parkinson's disease [40]. Also, the genetic modification of yeast to accelerate or decelerate the aging process is well-documented, including strains we characterized that vary in their production of reactive oxygen species (ROS) [41,42]. We will use these strains to examine how variation in oxidative stress affects Sod1 modification as cells age. Such studies can be easily performed since yeast cells rapidly age and data can be collected at numerous time points from independent cultures. Additionally, to establish if strains expressing Sod1-GFP can be used as indicators of Sod1 aggregation with age (Fig. 5), we will compare aggregation of wild-type protein with its GFP fusion to determine how the tag influences this process.

Conclusions

PTMs associated with protein misfolding have not been systematically investigated in the cellular environment. By combining SEC with high-performance LC–MS/MS, we discovered that oxidation of residues critical for folding and activity leads to HMW Sod1 formation in stationary-phase yeast. Further detailed characterization of oxidized Sod1 and its aggregation in yeast will provide important insights into protein misfolding mechanisms driven by oxidative stress in aging cells.

Conflict of interest

The authors report no conflicts of interest in this work.

Acknowledgments

This work was performed with funding from the Natural Sciences and Engineering Research Council of Canada (NSERC) and Concordia University. A.M.E holds a Concordia University Research Chair. D.M. acknowledges doctoral scholarship from FRQ-NT (Quebec) and additional awards from Concordia University and PROTEO, the FRQ-NT Network for Research on Protein Function, Structure, and Engineering.

Supplementary material

Supplementary material associated with this article can be found, in the online version, at doi:10.1016/j.redox.2014.03.005.

References

[1] H. Kawamata, G. Manfredi, Import, maturation, and function of SOD1 and its copper chaperone CCS in the mitochondrial intermembrane space, Antioxidants & Redox Signaling 13 (2010) 1375–1384. http://dx.doi.org/10.1089/ars.2010.3212, 20367259.

[2] L.A. Sturtz, K. Diekert, L.T. Jensen, R. Lill, V.C. Culotta, A fraction of yeast Cu, Zn-superoxide dismutase and its metallochaperone, CCS, localize to the intermembrane space of mitochondria. A physiological role for SOD1 in guarding against mitochondrial oxidative damage, Journal of Biological Chemistry 276 (2001) 38084–38089, 11500508.

[3] V.D. Longo, E.B. Gralla, J.S. Valentine, Superoxide dismutase activity is essential for stationary phase survival in *Saccharomyces cerevisiae*. Mitochondrial production of toxic oxygen species in vivo, Journal of Biological Chemistry 271 (1996) 12275–12280. http://dx.doi.org/10.1074/jbc.271.21.12275, 8647826.

[4] V.K. Mulligan, A. Chakrabartty, Protein misfolding in the late-onset neurodegenerative diseases: common themes and the unique case of amyotrophic lateral sclerosis, Proteins 81 (2013) 1285–1303. http://dx.doi.org/10.1002/prot.24285, 23508986.

[5] J. Choi, H.D. Rees, S.T. Weintraub, A.I. Levey, L.S. Chin, L. Li, Oxidative modifications and aggregation of Cu,Zn-superoxide dismutase associated with Alzheimer and Parkinson diseases, Journal of Biological Chemistry 280 (2005) 11648–11655. http://dx.doi.org/10.1074/jbc.M414327200, 15659387.

[6] O. Abel, J.F. Powell, P.M. Andersen, A. Al-Chalabi, ALSoD:a user-friendly online bioinformatics tool for amyotrophic lateral sclerosis genetics, Human Mutation 33 (2012) 1345–1351. http://dx.doi.org/10.1002/humu.22157, 22753137.

[7] J.S. Valentine, P.J. Hart, Misfolded CuZnSOD and amyotrophic lateral sclerosis, Proceedings of the National Academy of Sciences of the United States of America 100 (2003) 3617–3622. http://dx.doi.org/10.1073/pnas.0730423100, 12655070.

[8] J.S. Valentine, P.A. Doucette, S.Z. Potter, Copper–zinc superoxide dismutase and amyotrophic lateral sclerosis, Annual Review of Biochemistry 74 (2005) 563–593. http://dx.doi.org/10.1146/annurev.biochem.72.121801.161647, 15952898.

[9] A. Stieber, J.O. Gonatas, N.K. Gonatas, Aggregates of mutant protein appear progressively in dendrites, in periaxonal processes of oligodendrocytes, and in neuronal and astrocytic perikarya of mice expressing the SOD1(G93A) mutation of familial amyotrophic lateral sclerosis, Journal of the Neurological Sciences 177 (2000) 114–123. http://dx.doi.org/10.1016/S0022-510X(00)00351-8, 10980307.

[10] L.I. Grad, W.C. Guest, A. Yanai, E. Pokrishevsky, M.A. O'Neill, E. Gibbs, et al, Intermolecular transmission of superoxide dismutase 1 misfolding in living cells, Proceedings of the National Academy of Sciences of the United States of America 108 (2011) 16398–16403. http://dx.doi.org/10.1073/pnas.1102645108, 21930926.

[11] R. Rakhit, P. Cunningham, A. Furtos-Matei, S. Dahan, X.F. Qi, J.P. Crow, et al, Oxidation-induced misfolding and aggregation of superoxide dismutase and its implications for amyotrophic lateral sclerosis, Journal of Biological Chemistry 277 (2002) 47551–47556. http://dx.doi.org/10.1074/jbc.M207356200, 12356748.

[12] R. Rakhit, J.P. Crow, J.R. Lepock, L.H. Kondejewski, N.R. Cashman, A. Chakrabartty, Monomeric Cu,Zn-superoxide dismutase is a common misfolding intermediate in the oxidation models of sporadic and familial amyotrophic lateral sclerosis, Journal of Biological Chemistry 279 (2004) 15499–15504. http://dx.doi.org/10.1074/jbc.M313295200, 14734542.

[13] A. Kerman, H. Liu, S. Croul, J. Bilbao, E. Rogaeva, L. Zinman, et al, Amyotrophic lateral sclerosis is a non-amyloid disease in which extensive misfolding of SOD1 is unique to the familial form, Acta Neuropathologica 119 (2010) 335–344. http://dx.doi.org/10.1007/s00401-010-0646-5, 20111867.

[14] N. Brandes, H. Tienson, A. Lindemann, V. Vitvitsky, D. Reichmann, R. Banerjee, et al, Time line of redox events in aging postmitotic cells, ELife 2 (2013) e00306, 23390587.

[15] B.S. Berlett, E.R. Stadtman, Protein oxidation in aging, disease, and oxidative stress, Journal of Biological Chemistry 272 (1997) 20313–20316. http://dx.doi.org/10.1074/jbc.272.33.20313, 9252331.

[16] K. Uchida, S. Kawakishi, Identification of oxidized histidine generated at the active site of Cu,Zn-superoxide dismutase exposed to H_2O_2. Selective generation of 2-oxo-histidine at the histidine 118, Journal of Biological Chemistry 269 (1994) 2405–2410, 8300566.

[17] R.H. Gottfredsen, U.G. Larsen, J.J. Enghild, S.V. Petersen, Hydrogen peroxide induce modifications of human extracellular superoxide dismutase that results in enzyme inhibition, Redox Biology 1 (2013) 24–31. http://dx.doi.org/10.1016/j.redox.2012.12.004, 24024135.

[18] D.C. Ramirez, S.E.G. Mejiba, R.P. Mason, Mechanism of hydrogen peroxide-induced Cu,Zn-superoxide dismutase-centered radical formation as explored by immuno-spin trapping: the role of copper- and carbonate radical anion-mediated oxidations, Free Radical Biology & Medicine 38 (2005) 201–214. http://dx.doi.org/10.1016/j.freeradbiomed.2004.10.008, 15607903.

[19] K. Ranguelova, D. Ganini, M.G. Bonini, R.E. London, R.P. Mason, Kinetics of the oxidation of reduced Cu,Zn-superoxide dismutase by peroxymonocarbonate, Free Radical Biology & Medicine 53 (2012) 589–594. http://dx.doi.org/10.1016/j.freeradbiomed.2012.04.029, 22569304.

[20] B.R. Roberts, J.A. Tainer, E.D. Getzoff, D.A. Malencik, S.R. Anderson, V.C. Bomben, et al, Structural characterization of zinc-deficient human superoxide dismutase and implications for ALS, Journal of Molecular Biology 373 (2007) 877–890. http://dx.doi.org/10.1016/j.jmb.2007.07.043, 17888947.

[21] T. Kurahashi, A. Miyazaki, S. Suwan, M. Isobe, Extensive investigations on oxidized amino acid residues in H_2O_2-treated Cu,Zn-SOD protein with LC-ESI–Q-TOF-MS, MS/MS for the determination of the copper-binding site, Journal of the American Chemical Society 123 (2001) 9268–9278. http://dx.doi.org/10.1021/ja015953r, 11562208.

[22] S.C. Barber, P.J. Shaw, Oxidative stress in ALS: key role in motor neuron injury and therapeutic target, Free Radical Biology & Medicine 48 (2010) 629–641. http://dx.doi.org/10.1016/j.freeradbiomed.2009.11.018, 19969067.

[23] E. Linares, L.V. Seixas, J.N. dos Prazeres, F.V.L. Ladd, A.A.B.L. Ladd, A.A. Coppi, et al, Tempol moderately extends survival in a hSOD1(G93A) ALS rat model by inhibiting neuronal cell loss, oxidative damage and levels of non-native hSOD1(G93A) forms, PloS One 8 (2013) e55868. http://dx.doi.org/10.1371/journal.pone.0055868, 23405225.

[24] E. Ghezzo-Schoneich, S.W. Esch, V.S. Sharov, C. Schoneich, Biological aging does not lead to the accumulation of oxidized Cu,Zn-superoxide dismutase in the liver of F344 rats, Free Radical Biology & Medicine 30 (2001) 858–864. http://dx.doi.org/10.1016/S0891-5849(01)00473-7, 11295528.

[25] M.H. Barros, F.M.d. Cunha, G.A. Oliveira, E.B. Tahara, A.J. Kowaltowski, Yeast as a model to study mitochondrial mechanisms in ageing, Mechanisms of Ageing and Development 131 (2010) 494–502. http://dx.doi.org/10.1016/j.mad.2010.04.008, 20450928.

[26] P.W. Piper, Long-lived yeast as a model for ageing research, Yeast (Chichester, England) 23 (2006) 215–226. http://dx.doi.org/10.1002/yea.1354, 16498698.

[27] V.D. Longo, G.S. Shadel, M. Kaeberlein, B. Kennedy, Replicative and chronological aging in *Saccharomyces cerevisiae*, Cell Metabolism 16 (2012) 18–31. http://dx.doi.org/10.1016/j.cmet.2012.06.002, 22768836.

[28] P. Fabrizio, V.D. Longo, The chronological life span of *Saccharomyces cerevisiae*, Aging Cell 2 (2003) 73–81. http://dx.doi.org/10.1046/j.1474-9728.2003.00033.x, 12882320.

[29] V. Khurana, S. Lindquist, Modelling neurodegeneration in *Saccharomyces cerevisiae*: why cook with Baker's yeast? Nature Reviews. Neuroscience 11 (2010) 436–449. http://dx.doi.org/10.1038/nrn2809, 20424620.

[30] H. Jiang, A.M. English, Phenotypic analysis of the ccp1Delta and ccp1Delta-ccp1W191F mutant strains of *Saccharomyces cerevisiae* indicates that cytochrome c peroxidase functions in oxidative-stress signaling, Journal of Inorganic Biochemistry 100 (2006) 1996–2008. http://dx.doi.org/10.1016/j.jinorgbio.2006.07.017, 17011626.

[31] M.M. Bradford, A rapid and sensitive method for the quantitation of microgram quantities of protein utilizing the principle of protein-dye binding, Analytical Biochemistry 72 (1976) 248–254. http://dx.doi.org/10.1016/0003-2697(76)90527-3, 942051.

[32] C.J. Weydert, J.J. Cullen, Measurement of superoxide dismutase, catalase and glutathione peroxidase in cultured cells and tissue, Nature Protocols 5 (2010) 51–66. http://dx.doi.org/10.1038/nprot.2009.197, 20057381.

[33] A. Tiwari, L.J. Hayward, Familial amyotrophic lateral sclerosis mutants of copper/zinc superoxide dismutase are susceptible to disulfide reduction, Journal of Biological Chemistry 278 (2003) 5984–5992. http://dx.doi.org/10.1074/jbc.M210419200, 12458194.

[34] M.J. Lindberg, J. Normark, A. Holmgren, M. Oliveberg, Folding of human superoxide dismutase: disulfide reduction prevents dimerization and produces marginally stable monomers, Proceedings of the National Academy of Sciences of the United States of America 101 (2004) 15893–15898. http://dx.doi.org/10.1073/pnas.0403979101, 15522970.

[35] S. Ghosh, B. Willard, S.A. Comhair, P. Dibello, W. Xu, S. Shiva, et al, Disulfide bond as a switch for copper–zinc superoxide dismutase activity in asthma, Antioxidants & Redox Signaling 18 (2013) 412–423, 22867017.

[36] S.M. Lynch, S.A. Boswell, W. Colon, Kinetic stability of Cu/Zn superoxide dismutase is dependent on its metal ligands: implications for ALS, Biochemistry 43 (2004) 16525–16531. http://dx.doi.org/10.1021/bi048831v, 15610047.

[37] M. Synofzik, D. Ronchi, I. Keskin, A.N. Basak, C. Wilhelm, C. Gobbi, et al, Mutant superoxide dismutase-1 indistinguishable from wild-type causes ALS, Human Molecular Genetics 21 (2012) 3568–3574. http://dx.doi.org/10.1093/hmg/dds188.

[38] C.M.J. Higgins, C.W. Jung, Z.S. Xu, ALS-associated mutant SOD1G93A causes mitochondrial vacuolation by expansion of the intermembrane space and by involvement of SOD1 aggregation and peroxisomes, BMC Neuroscience 4 (2003) 16. http://dx.doi.org/10.1186/1471-2202-4-16, 12864925.

[39] E.L. Bastow, C.W. Gourlay, M.F. Tuite, Using yeast models to probe the molecular basis of amyotrophic lateral sclerosis, Biochemical Society Transactions 39 (2011) 1482–1487. http://dx.doi.org/10.1042/BST0391482, 21936838.

[40] D.F. Tardiff, N.T. Jui, V. Khurana, M.A. Tambe, M.L. Thompson, C.Y. Chung, et al, Yeast reveal a "druggable" Rsp5/Nedd4 network that ameliorates alpha-synuclein toxicity in neurons, Science (New York, NY) 342 (2013) 979–983. http://dx.doi.org/10.1126/science.1245321, 24158909.

[41] D. Martins, M. Kathiresan, A.M. English, Cytochrome c peroxidase is a mitochondrial heme-based H_2O_2 sensor that modulates antioxidant defense, Free Radical Biology & Medicine 65 (2013) 541–551.

[42] D. Martins, V.I. Titorenko, A.M. English, Cells with impaired mitochondrial H_2O_2 sensing generate less •OH radicals and live longer, Antioxidants and Redox Signaling (2014). http://dx.doi.org/10.1089/ars.2013.5575, in press.